



# LUND UNIVERSITY

## The effect of defects at the steel - concrete interface, exposure regime and cement type on pitting corrosion in concrete

Sandberg, Paul

1998

[Link to publication](#)

*Citation for published version (APA):*

Sandberg, P. (1998). *The effect of defects at the steel - concrete interface, exposure regime and cement type on pitting corrosion in concrete*. (Report TVBM; Vol. 3081). Division of Building Materials, LTH, Lund University.

*Total number of authors:*

1

### General rights

Unless other specific re-use rights are stated the following general rights apply:

Copyright and moral rights for the publications made accessible in the public portal are retained by the authors and/or other copyright owners and it is a condition of accessing publications that users recognise and abide by the legal requirements associated with these rights.

- Users may download and print one copy of any publication from the public portal for the purpose of private study or research.
- You may not further distribute the material or use it for any profit-making activity or commercial gain
- You may freely distribute the URL identifying the publication in the public portal

Read more about Creative commons licenses: <https://creativecommons.org/licenses/>

### Take down policy

If you believe that this document breaches copyright please contact us providing details, and we will remove access to the work immediately and investigate your claim.

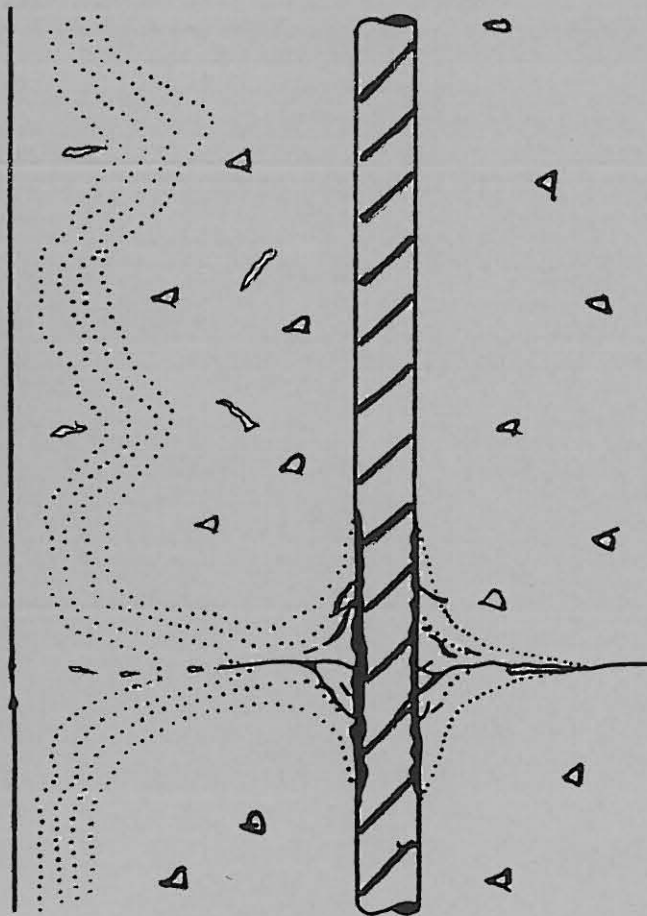
LUND UNIVERSITY

PO Box 117  
221 00 Lund  
+46 46-222 00 00



# The effect of defects at the steel – concrete interface, exposure regime and cement type on pitting corrosion in concrete

Paul Sandberg





# **The effect of defects at the steel – concrete interface, exposure regime and cement type on pitting corrosion in concrete**

**Paul Sandberg**

ISRN LUTVDG/TVBM--98/3081--SE(1-18)  
ISSN 0348-7911 TVBM

Lund Institute of Technology  
Division of Building Materials  
Box 118  
S-221 00 Lund, Sweden

Telephone: 46-46-2227415  
Telefax: 46-46-2224427

## **PREFACE**

This report is a compilation of results from studies of the effects of defects at the steel – concrete interface, the exposure regime, and the cement type, on the initiation of pitting corrosion in specially designed concrete corrosion cells. A compilation of all threshold levels calculated is available in Appendix A.

A standard corrosion cell has been used in this study, as developed by Hans Arup Consult and Henrik Sørensen, AEC Consulting Engineers, Denmark, in cooperation with the present author. All corrosion cells have been manufactured at AEC Consulting Engineers, Denmark using electrical components selected and customized by Hans Arup Consult and Tord Lundgren, Lund Institute of Technology.

The exposure tests in this study have been carried out by the present author at Lund Institute of Technology, Division of Building Materials and at the Träslövsläge Marine Field Station, and by Henrik Sørensen at AEC Consulting Engineers. The datalogger system used for automatic registration of steel potentials and corrosion rates was developed by Tord Lundgren, Lund Institute of Technology.

The procedure for sampling concrete dust for the analysis of total chloride profiles was developed by Jens Frederiksen and Henrik Sørensen at AEC Consulting Engineers, Denmark. Total chloride profiles have been measured at Lund Institute of Technology, AEC Consulting Engineers and the Swedish National Testing and Research Institute, following a procedure for analysis of total chloride content by weight of binder in concrete as developed by Tang Luping, then at Chalmers Institute of Technology.

Visual studies of the corrosion attack on steel electrodes and of the microstructure of concrete at the steel – concrete interface were carried out by Henrik Sørensen at AEC Consulting Engineers and by the present author.

The analysis work has been planned and coordinated by the author and financed by Cementa AB and AEC Consulting Engineers A/S.

Lund in April, 1998.

Paul Sandberg

UNIVERSITY OF LUND  
LUND INSTITUTE OF TECHNOLOGY  
DIVISION OF BUILDING MATERIALS

Report TVBM-3081

Lund, 1998

## The effects of defects at the steel-concrete interface, exposure regime and cement type on pitting corrosion in concrete

P. Sandberg

*Cementa AB, Box 300 22, S- 200 61 Malmö, Sweden*

*and Division of Building Materials, Lund Institute of Technology, S-222 21 Lund, Sweden*

### Abstract

The effects of defects at the steel-concrete interface, the exposure regime, and the cement type, on the initiation of pitting corrosion in specially designed concrete corrosion cells were investigated. Concrete/mortar corrosion cells with cast-in mild steel electrodes representing the reinforcement were exposed for wetting-drying cycles or submerged in NaCl solution. Parallel field exposure testes were carried out in sea water. The microstructure of the steel-concrete interface was altered by introduction of a filter paper on the steel surface, by bending of the steel electrode and by compaction voids or cracks formed at or close to the steel surface.

The results indicated that corrosion in most cases was initiated in deformed parts of steel electrodes. Defects introduced at or close to the steel surface had a strong negative influence on the chloride threshold for concrete exposed to wetting and drying and for field exposed concrete exposed submerged or in the splash zone, but not for submerged laboratory exposed concrete.

The negative effect of filter paper and voids or cracks at the steel surface was stronger for slag cement concrete as compared to concrete with sulphate resisting Portland cement with 0 or 5 % silica fume in the binder.

The results support the idea that chloride induced pitting corrosion of steel in concrete is enforced mainly under conditions of variable exposure conditions and in the presence of defects at the steel surface. The results also indicate that reinforced slag cement concrete is more sensitive to the formation of, and the effect of, cracks and other defects at the steel – concrete interface as compared to concrete based on sulfate resisting cement with 0 or 5 % silica fume in the binder.

## **1. INTRODUCTION**

Chloride induced reinforcement corrosion is one of the most common durability problem associated with modern good quality reinforced concrete structures exposed to a marine environment or to de-icing salts. The time to corrosion initiation depends on i) how fast chloride ions penetrate the concrete cover to reach the reinforcement, and ii) the critical chloride concentration needed for depassivation of the steel reinforcement. This report is a compilation of results from studies of the effects of defects at the steel-concrete interface, the exposure regime, and the cement type, on the initiation of pitting corrosion in specially designed concrete corrosion cells. Compilations of numerical data on the chloride thresholds found in field exposed reinforced concrete slabs and in field- and laboratory exposed corrosion cells can be found in /1,2/ and in Appendix A.

## **2. THE CHLORIDE THRESHOLD LEVEL**

### 2.1 General

The chloride threshold level refers to the concentration of chlorides required to destroy the normal passivity of steel in concrete. The chloride threshold reflects the critical concentration of free chloride and hydroxide ions in the concrete pore solution at an emerging corrosion pit on the reinforcement, but it is for practical reasons /3/ often expressed as the total chloride content by weight of binder.

### 2.2 Definition of the chloride threshold

In this study the chloride threshold was defined as the mass ratio of measured total (bound + free) aggressive substance (chloride) and measured inhibiting substance (binder) necessary to maintain active corrosion in a pit. The corrosion process was considered active if the corrosion current was  $> 1 \mu\text{A}/\text{cm}^2$ .

### 2.3 Purpose of study

Chloride threshold levels reported in the literature are confusing as they vary extensively depending on the experimental methods, the exposure conditions, the concrete quality and the cement type used /1,3/. The purpose of this study was to isolate and demonstrate the importance of defects at, or close to, the steel surface, on the mechanisms of corrosion initiation in chloride exposed concrete containing steel electrodes as model reinforcement. The effects of exposure regime and cement type were also studied.

## **3. FACTORS AFFECTING THE IDENTIFICATION AND USE OF CHLORIDE THRESHOLD LEVELS**

### 3.1 General

The chloride threshold level for mild steel in a given concrete quality seems to depend on both the micro structure /4/ and the micro climate /1-3/ at the concrete-steel interface.

### 3.2 The effect of micro structure at the concrete - steel interface

The chloride threshold level for mild steel exposed to alkaline chloride solutions reflecting typical concrete pore solutions are often lower than the corresponding threshold level for steel in concrete. The difference can be orders of magnitude /5/. The reasons for the improved chloride resistance for steel in concrete as compared to steel in alkaline solutions, are not fully understood. Experimental work by Yonezawa et al /4/, including variations in the bonding between the steel and the cement matrix, have indicated that the effect of physical adhesion between cement hydrates and iron oxides formed on the steel surface is important. It was concluded that the formation of voids at the steel-mortar interface is a necessary condition for active corrosion to start in water saturated concrete containing a moderate chloride content. Furthermore, observations of a protective effect of calcium hydroxide precipitated at the steel surface were reported. The protective effect of calcium hydroxide was attributed to the dissolution of calcium hydroxide crystals close to emerging pits, thereby preventing the pH drop required for the further propagation of the corrosion pit.

Mammoliti et al /6/ on the other hand found that the tendency for pitting of steel exposed to alkaline solutions was controlled by the surface roughness of the steel and by the pH of the solution. At pH 13.3 continued pitting was not possible to initiate on any steel surface independently of the surface roughness. It was suggested that testing of steel in solutions is not representative for the inhomogeneous material concrete. Concrete is likely to exhibit local variations in the pH of the pore solution at the steel surface as opposed to well stirred solutions.

### 3.3 The effect of micro climate at the concrete - steel interface

Some evidence exists that the chloride threshold levels vary with the exposure conditions, especially with the moisture state /2,7,8/. Very high threshold levels have been found for steel in concrete exposed fully submerged in the laboratory with no changes in the exposure regime /2/. A varying moisture state at the depth of the reinforcement caused by wetting and drying of concrete has been suggested to result in a substantially lower threshold level /7,8,9/, which was confirmed by the findings in /2/. The results in /1,2/ confirmed that a more stable micro environment, as achieved by an increased cover size and/or a lower w/c ratio, or by a non-varying exposure condition, may result in a higher chloride threshold.

## **4. EXPERIMENTAL**

### 4.1 Corrosion cells for testing the effect of various defects at the steel-concrete interface

A standard corrosion cell for testing of chloride thresholds in concrete /11/ was developed by Hans Arup, formerly at the Danish Corrosion Centre, in co-operation with Henrik Sørensen at AEC, Denmark and the present author at Cementa, Sweden. The test unit consists of 20 U-shaped smooth Ø 8 mm mild steel electrodes, 2 titanium mesh counter electrodes and a MnO<sub>2</sub> reference electrode which were very accurately positioned into a cement based precast specimen holder as shown in Figure 1. The MnO<sub>2</sub> reference electrode reads + 142 mV SCE. Some of the electrodes were connected to a potentiostat and kept under potentiostatic control according to Table 3-5.



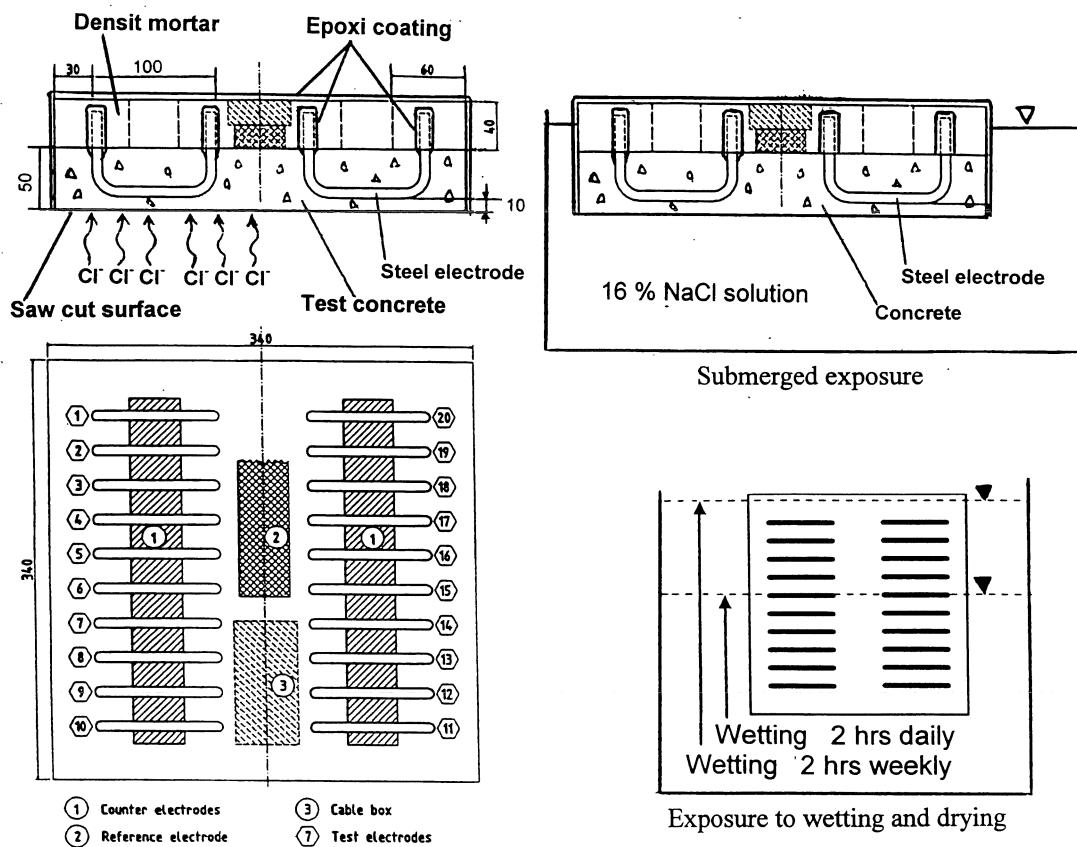


Figure 1. Standard corrosion cell. All measures are given in millimetres [11].

The U-shaped steel electrodes have epoxy coated legs facing away from the exposed surface in order to prevent corrosion initiation on the legs. The  $MnO_2$  reference electrode and the titanium mesh counter electrode were cast into mortar bars before assembling the standard unit. The design minimises errors due to IR-drops in the test concrete.

The steel electrodes were embedded into the concrete or mortar to be tested. The placing and compacting of concrete were carried out carefully as described in [12]. After demoulding and moist curing for 14 days the concrete surface to be exposed was cut open using a large water-cooled diamond saw to obtain a cover to the steel electrodes of nominally 10 mm. A chloride proof coating was applied to the test unit on all sides except the saw-cut face to be exposed.

Nine "dummy" concrete specimens were made from the cut off concrete plate. These specimens were handled in exactly the same manner as the test unit containing the embedded steel. All surfaces were coated except for the surface opponent to the exposed surface on the test unit. The test unit and the dummy concrete specimens were then stored in a saturated calcium hydroxide solution at room temperature for 2 weeks prior to the saline exposure.

Steel-, counter- and reference electrodes were connected to a datalogger for monitoring the corrosion activity. A potentiostat was available for potentiostatic control of steel electrodes before the corrosion initiation.

#### 4.2 Introduction of artificially produced defects at the steel-concrete interface

A standard filter paper was applied on the surface on some steel electrodes according to Figure 2 and Table 3-5, with the purpose to produce artificial defects at the steel-concrete interface, following the procedure in [3] by Yonezawa et al. The filter paper used was a Schleicher & Schuell, Filter Paper Circles no. 589-1, Black Ribbon, Ashless, Ø110 mm, Ref. No. 300 010. The filter paper was mounted in 2 layers on the steel surface and fixed by a 0.40 mm nylon string. The filter paper was soaked in a 0.4 M KOH solution immediately before the casting of concrete or mortar on top of the filter paper coated steel electrodes. The KOH soaked filter paper was used with the aim to simulate a situation with the steel in contact with a simulated pore solution but without physical contact with cement hydrates.

#### 4.3 Introduction of compaction voids at the steel-concrete interface

All concrete mixes were cast, compacted and cured in a similar way as recommended in [12]. A total of 34 electrodes were found to be affected by visible compaction voids or cracks, approximately 0.1-0.5 mm wide, at the steel surface. 17 or about 50 % of these electrodes were found in slag cement concrete.

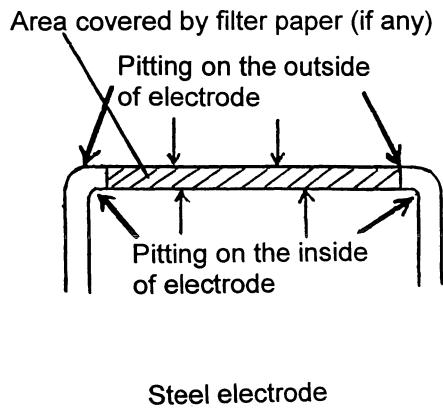
#### 4.4 Registration of corrosion activity

The corrosion activity in electrodes under potentiostatic control was recorded by a datalogger on a hourly basis by measuring the electrical current needed to maintain the steel electrodes at their controlled potentials. The initiation of active corrosion was detected by an increase in the current to more than 100  $\mu$ A. After initiation the potentiostatic control was removed and the steel electrode was allowed to corrode freely, at the same exposure condition as before, with the potential recorded by the datalogger.

The corrosion activity in electrodes not under potentiostatic control was recorded by a datalogger simply by recording the steel potentials. Corrosion initiation was indicated by a shift in the order of 200-500 mV to a more negative potential.

#### 4.5 Evaluation of location and size of corrosion pits

At the end of exposure of a test cell, electrodes were removed from the cell and carefully examined visually in order to confirm the position and the approximate size of the corrosion pit. The evaluation was carried out as indicated in Figure 2.



Degree of corrosion	Description of corrosion pit
0	None
1	Very small pit, 0-1 % of steel surface, only surface corrosion
2	Small pit, 1-10 % of steel surface, max 0.5 mm deep
3	Corrosion in 10-50 % of steel surface, max 1.0 mm deep
4	Corrosion in 50-100 % of steel surface, > 1.0 mm deep

Figure 2. Evaluation of location and size of corrosion pits

#### 4.6 Evaluation of defects in the concrete microstructure close to the steel surface

The concrete surrounding each electrode was examined for the existence of visible cracks or voids close to the steel electrode. This was aided by a visual examination of the distribution of chlorides in the surrounding concrete, by spraying freshly cut surfaces with a 0.1 M  $\text{AgNO}_3$  solution. The formation of light grey  $\text{AgCl}$  precipitate at chloride rich cracks or voids provided a visual indication of chloride rich areas in concrete surrounding the steel electrodes.

#### 4.7 Analysis of chloride- and binder profiles

Total chloride- and binder profiles were analysed at the first corrosion initiation. Total chloride profiles were also analysed after corrosion initiation in 25% and 50% of the steel electrodes and after 2 years of exposure. The total chloride- and binder profiles were analysed on “dummy” concrete with no cast in steel electrodes.

The concrete cover was abraded from the exposed surface and inwards in steps of 1 mm using a diamond tool according to the Nordic standard NT Build 443 /13/. The pulverized samples were analyzed for total chloride content according to AASHTO T 260-A, by potentiometric titration using a chloride ion selective electrode and a silver nitrate solution of 0.01 N.

After chloride titration, 5 ml of 1:2 diluted triethanolamine was added to the sample solution and the pH value was adjusted to  $\text{pH} > 12$  using sodium hydroxide. The calcium content was determined by potentiometric titration using a calcium ion selective electrode and a 0.1 N EDTA solution /14/. Since the aggregate contained no acid soluble calcium, the binder content in each 1 mm fraction of concrete was calculated from the measured calcium content in each fraction. The result was presented as total chloride by weight of binder for each 1 mm fraction.

#### 4.8 Calculation of chloride threshold

The location of the corrosion pit (at the steel electrode facing the exposed concrete surface) was used to measure the exact distance from the exposed concrete surface to the steel surface at the pit. The measured total chloride profiles at various exposure ages were then used to extrapolate the total chloride content at the depth of the corrosion pit at the time of corrosion initiation.

#### 4.9 Types of binder used

Three different binder types, sulfate resisting Portland cement (SRPC), sulfate resisting Portland cement with 5 % silica fume, and slag cement with 50 % slag interground with Portland cement, were used as shown in Table 1.

**Table 1.** Details of cementing materials used

Material		Sulfate resisting Portland cement (SRPC)	Slag cement 50 % slag interground	Silica fume (SF)
Fineness - % passing	45 $\mu\text{m}$	85.9	100	100
	20 $\mu\text{m}$	51.3	72.0	
	10 $\mu\text{m}$	33.1	45.3	
	5 $\mu\text{m}$	19.5	33.8	
	1 $\mu\text{m}$	3.8	8.2	
Specific surface $\text{m}^2/\text{kg}$	Blaine	300	410	23 000
	BET			
Compressive Strength of standard 40 mm mortar cubes, MPa	1 day	10.1	4.0	
	7 days	35.6	29.7	
	28 days	56.2	49.8	
Chemical analysis %	CaO	63.8	43.3	0.4
	SiO <sub>2</sub>	22.8	28.5	94.2*
	Al <sub>2</sub> O <sub>3</sub>	3.5	11.9	0.62
	Fe <sub>2</sub> O <sub>3</sub>	4.7	1.1	0.95
	MgO	0.80	9.0	0.65
	SO <sub>3</sub>	1.9	4.7	0.33
	K <sub>2</sub> O	0.55	0.55	0.5
	Na <sub>2</sub> O	0.06	0.26	0.2
Loss of ignition	0.55	0	1.8	
Bouge potential compounds -%	C <sub>3</sub> S	51.5		
	C <sub>2</sub> S	25.5		
	C <sub>3</sub> A	1.3		
	C <sub>4</sub> AF	14.3		

\*amorphous silica content

#### 4.10 Concrete/mortar mix designs

Details of the concrete or mortar mixes are shown in Table 2.

**Table 2.** Details of concrete/mortar mixes used in corrosion cell tests

Mix No.	Material	Cover mm	SRPC kg/m <sup>3</sup>	Slag cem. kg/m <sup>3</sup>	Silica fume kg/m <sup>3</sup>	Sand 0-2 mm kg/m <sup>3</sup>	Sand 0-4 mm kg/m <sup>3</sup>	Aggr. 0-8 mm kg/m <sup>3</sup>	Aggr. 8-16 mm kg/m <sup>3</sup>	w/c ratio *	Air cont. vol %
1	Concrete	10	330	0	0	-	645	189	1058	0.50	1.0
2	Concrete	10	435	0	0	760	-	970	-	0.41	2.1
3	Concrete	10	420	0	16	750	-	970	-	0.42	1.9
4	Concrete	10	0	435	0	755	-	965	-	0.40	1.4
5	Mortar	4-14	555	0	29	1440	-	0	-	0.40	-

\*w/c ratio defined as w/(C+SF). w = water, C = cement

#### 4.11 Exposure conditions

Corrosion cells with plain sulfate resisting portland cement (SRPC), sulfate resisting portland cement with 5 % silica fume, or slag cement were exposed to 3 different exposure regimes as indicated below. Some of the steel electrodes were kept under potentiostatic control as indicated by the voltages in Tables 3-5. "Free pot." denotes that no potential control was applied. "Defects" denotes whether previously described artificial filter paper defects were introduced or not.

1) Submerged at + 5 °C or room temperature in a 16 % NaCl solution for 2 years. Table 3 and Figure 1.

**Table 3.** Configuration of steel electrodes in concrete/mortar corrosion cells exposed submerged in a 16 % NaCl solution at room temperature or at + 5 °C in the laboratory.

Cell Label	Mix No.	Steel potentials (mV rel. MnO <sub>2</sub> )										Defects	Exp. temp.	
		free pot.	-450 mV	-350 mV	-250 mV	-200 mV	-150 mV	-100 mV	-50 mV	0 mV	+50 mV			
A-PC0.50	1 <sup>□</sup>	2*	2	2	2	2	2	2	2	2	2	2	none	+ 20 °C
B-PC0.41	2	4	4	4	none	none	none	4	none	none	4	4	yes**	+ 20 °C
C-PC0.41	2	4	4	4	none	none	none	4	none	none	4	4	yes**	+ 5 °C
D-SF0.42	3	4	4	4	none	none	none	4	none	none	4	4	yes**	+ 5 °C
E-SL0.40	4	4	4	4	none	none	none	4	none	none	4	4	yes**	+ 5 °C
F-mortPC	5	10	none	10	none	none	none	none	none	none	none	none	none	+ 5 °C

\* Figure denotes number of electrodes.

\*\* 2 electrodes with filter paper on the steel surface tested at each potential.

<sup>□</sup>Cell A-PC0.50 was exposed for 4 years.

2) Cycles of 2 hours wetting in a 16 % NaCl solution and 22 or 166 hours drying, at room temperature for a total exposure time of 8 months, Table 4 and Figure 1.

**Table 4.** Configuration of steel electrodes in concrete corrosion cells exposed to a 16 % NaCl solution and subjected to cyclic wetting and drying in the laboratory at room temperature.

		Steel potentials (mV rel MnO <sub>2</sub> )							
		12 hrs wetting - 6½ days drying				12 hrs wetting - 12 hrs drying			
		Free potential		-350 mV		Free potential		-350 mV	
Cell Label	Mix No.	Filter paper defects		Filter paper defects		Filter paper defects		Filter paper defects	
		Yes	No	Yes	No	Yes	No	Yes	No
K-PC0.41	2	5*	5	0	0	5	4	0	1
L-SF0.42	3	5	5	0	0	5	4	0	1
M-SL0.40	4	5	5	0	0	5	4	0	1

\* Figure denotes number of electrodes

3) Marine field exposure for 2 years, submerged and in the splash zone of a floating pontoon at the Träslövsläge Marine Field Station on the Swedish west coast, Table 5 and Figure 3.

**Table 5.** Configuration of steel electrodes in concrete corrosion cells field exposed at the Träslövsläge Marine field Station.

		Steel potentials (mV rel MnO <sub>2</sub> )							
		Submerged				Splash zone			
		Free potential		-350 mV		Free potential		-350 mV	
Cell Label	Mix No.	Filter paper defects		Filter paper defects		Filter paper defects		Filter paper defects	
		Yes	No	Yes	No	Yes	No	Yes	No
O-subPC0.41	2	8*	8	2	2	-	-	-	-
P-splaPC0.41	2	-	-	-	-	8	8	2	2
R-subSF0.42	3	8	8	2	2	-	-	-	-
S-splaSF0.42	3	-	-	-	-	8	8	2	2
T-subSL0.40	4	8	8	2	2	-	-	-	-
U-splaSL0.40	4	-	-	-	-	8	8	2	2

\* Figure denotes number of electrodes

A mortar corrosion cell with sulfate resisting portland cement and 5 % silica fume, w/c 0.4, was exposed submerged in the laboratory for 2 years at + 5 °C in a 16 % NaCl solution, Table 2. However, no corrosion was initiated although total chloride contents as high as 1.7 % were measured at the depth of the steel electrodes. All calculated threshold levels were given in /2/ and are shown in Appendix A.

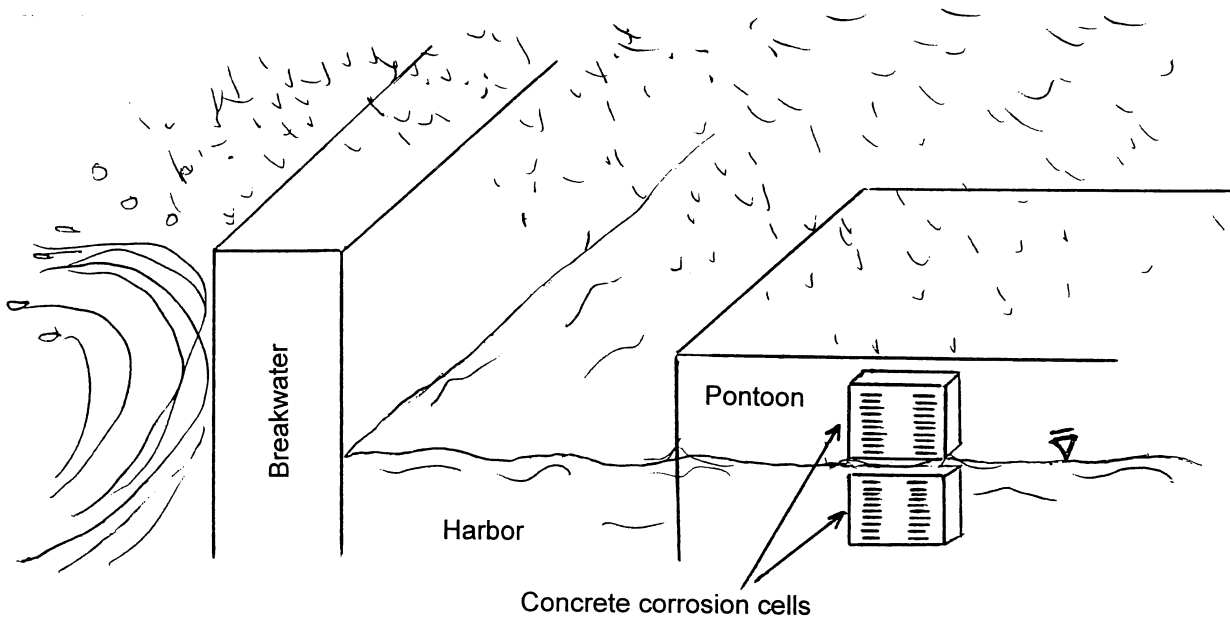


Figure 3. Exposure conditions for corrosion cells at the Träslövsläge Marine Field Station.

## 5. RESULTS

### 5.1 General

All calculated chloride thresholds with a discussion were presented in /2/. A compilation of data is available in Appendix A. Most of the results presented here focus on the effect of defects on the location and size of corrosion pits, and on the effects of exposure regime and cement type.

### 5.2 Presentation of results on the effect of defects on the location and size of corrosion pits

All results are presented in Appendix B.

Each concrete mix and exposure regime was evaluated separately, with the results presented as shown for slag cement concrete, w/c 0.40, exposed in the splash zone at the Träslövsläge Marine Field Station, in Figure 4.

The effect of defects was evaluated from the following indications:

- A) The location of the corrosion pit, Figure 2. Bending of hot rolled black steel causes deformation and possibly cracking of the scale in deformed zones, especially at the inside of a bend.

- B) The presence of corrosion pits in electrodes with artificial filter paper defects at the steel - concrete interface, relative to the presence of pits in electrodes without filter paper defects.
- C) The presence of visible compaction voids or cracks at the steel - concrete interface.

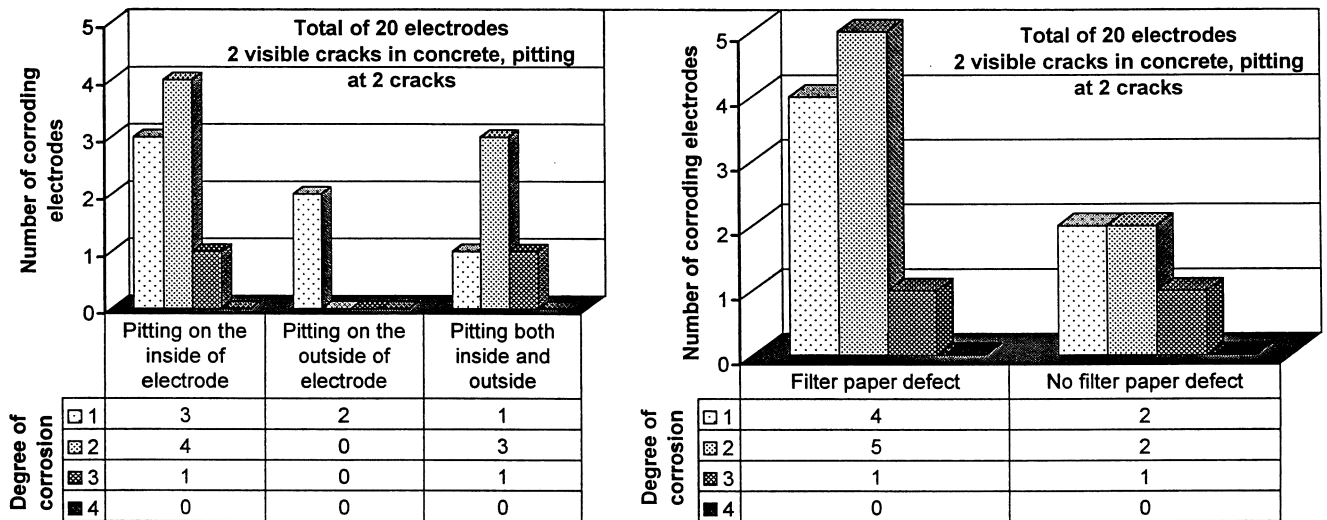


Figure 4. Presentation of results on the effect of defects on the location and size of corrosion pits.

### 5.3 Results from laboratory submerged exposure tests, concrete w/c 0.5 and 0.4

#### 5.3.1 Plain SRPC concrete w/c 0.50 exposed for 4 years

14 U-bend steel electrodes of a total of 20 started to corrode within 4 years of laboratory exposure of SRPC concrete w/c 0.50, submerged at room temperature in 16 % NaCl solution. The total chloride concentration at the depth of the corrosion pits were 2.5 to 3.0 % Cl by weight of binder after 4 years of exposure depending on the position of the corrosion pit. The visual examination revealed corrosion initiation in deformed parts of electrodes, Figure 5, at the inside of the U-shaped electrodes in 11 electrodes of 14, or in 75 % of the corroding electrodes.

A potential more negative than -100 mV SCE was necessary to prevent corrosion initiation in U-bend steel electrodes.



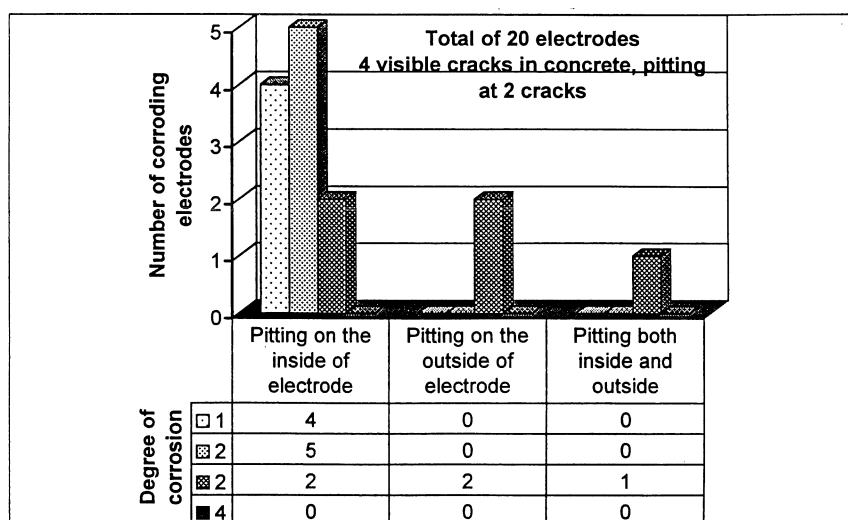


Figure 5. Evaluation of the location of corrosion pits in plain SRPC concrete exposed 4 years submerged in a 16 % NaCl solution at room temperature in the laboratory. No filter paper defects applied.

### 5.3.2 Concrete w/c 0.4 exposed for 2 years

For all other concrete corrosion cells submerged at the laboratory, only 6 of a total of 80 steel electrodes started to corrode within 2 years of exposure. 4 of the 6 corroding electrodes had corrosion initiation in the deformed zone at the inside of the U-shaped electrodes.

No corrosion at all was initiated in SRPC concrete with 5 % silica fume or slag cement concrete when exposed submerged in the laboratory at + 5 °C. On the other hand only 1.2 and 1.0 % Cl by weight of binder were measured in SRPC concrete with 5 % silica fume and slag cement concrete, respectively, at the depth of the steel electrodes. Only one electrode started to corrode in concrete exposed submerged in the laboratory at + 5 °C, in plain SRPC concrete, at 1.8 % Cl by weight of binder.

### 5.4 Results from laboratory wetting and drying exposure tests, concrete w/c 0.4

8 months of wetting and drying exposure (at room temperature) resulted in a substantial increase in the corrosion activity as compared to the 2 years submerged laboratory exposure tests (at room temperature or at + 5 °C). 6 of 8 electrodes with filter paper defects and / or compaction voids close to the steel surface started to corrode in the slag cement concrete already after a few months of exposure. On the other hand 2 of 11 electrodes with filter paper defects and / or compaction voids close to the steel surface started to corrode in SRPC concrete with 0 or 5 % silica fume in the binder. The results for all electrodes in concrete w/c 0.4 exposed for wetting and drying in the laboratory are summarised in Figure 6.

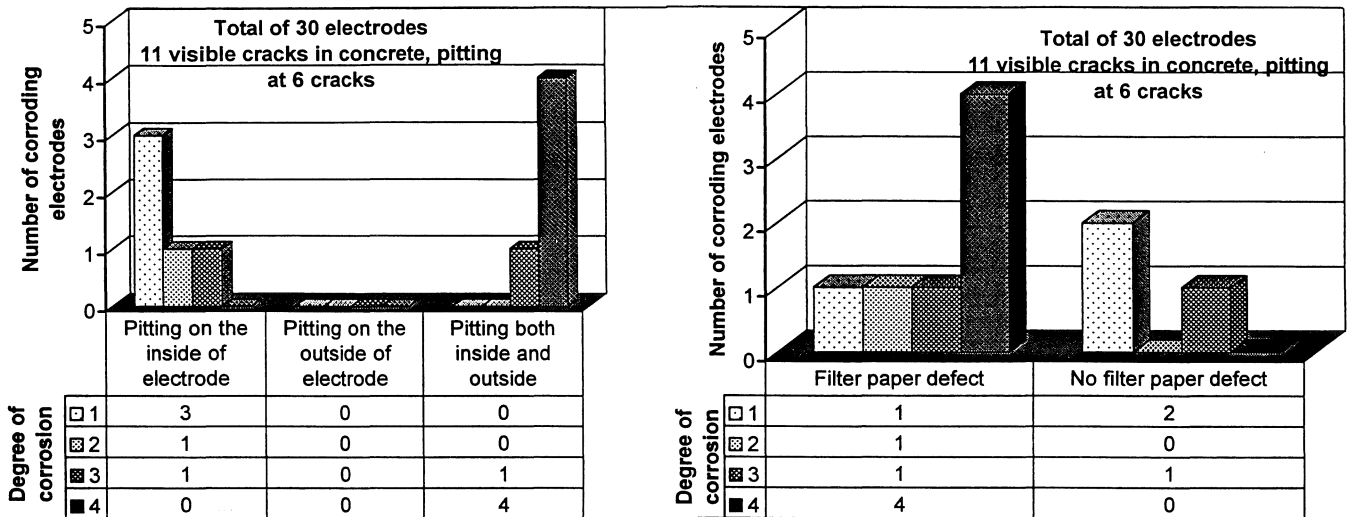


Figure 6. Evaluation of the location of corrosion pits in concrete w/c 0.4 exposed for wetting and drying for 8 months in a 16 % NaCl solution at room temperature in the laboratory.

### 5.5 Results from field exposure tests

#### 5.5.1 Exposure in the splash zone

17 of 40 electrodes started to corrode in the splash zone within 2 years of field exposure, Figure 7. 15 of the 17 corroding electrodes were found in slag cement concrete, with active corrosion in all electrodes with filter paper defects and / or compaction voids close to the steel surface. 5 of 10 electrodes in slag cement concrete without filter paper defects, voids or cracks were also corroding.

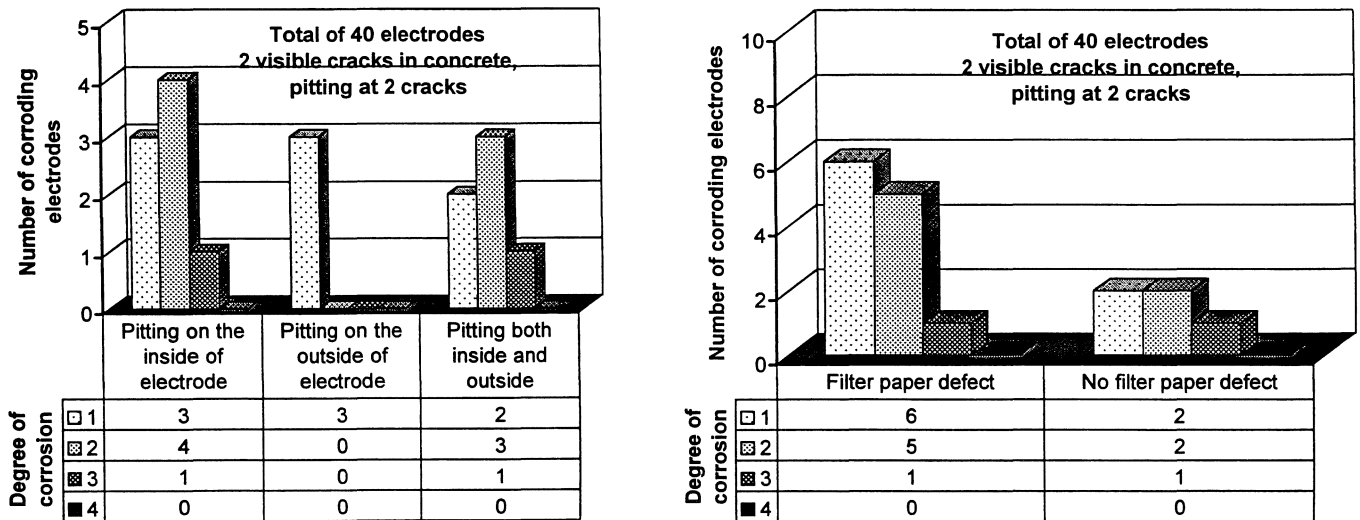


Figure 7. Evaluation of the location of corrosion pits in concrete w/c 0.4 exposed for 2 years in the splash zone at the Träslövsläge Marine Field Station.

### 5.5.2 Exposure in the submerged zone

11 of 60 electrodes started to corrode in the submerged zone within 2 years of field exposure, Figure 8. 8 of the 11 corroding electrodes were found in slag cement concrete, with active corrosion in 7 of 12 electrodes with filter paper defects and / or compaction voids close to the steel surface. 1 of 8 electrodes in slag cement concrete without filter paper defects, voids or cracks was also corroding.

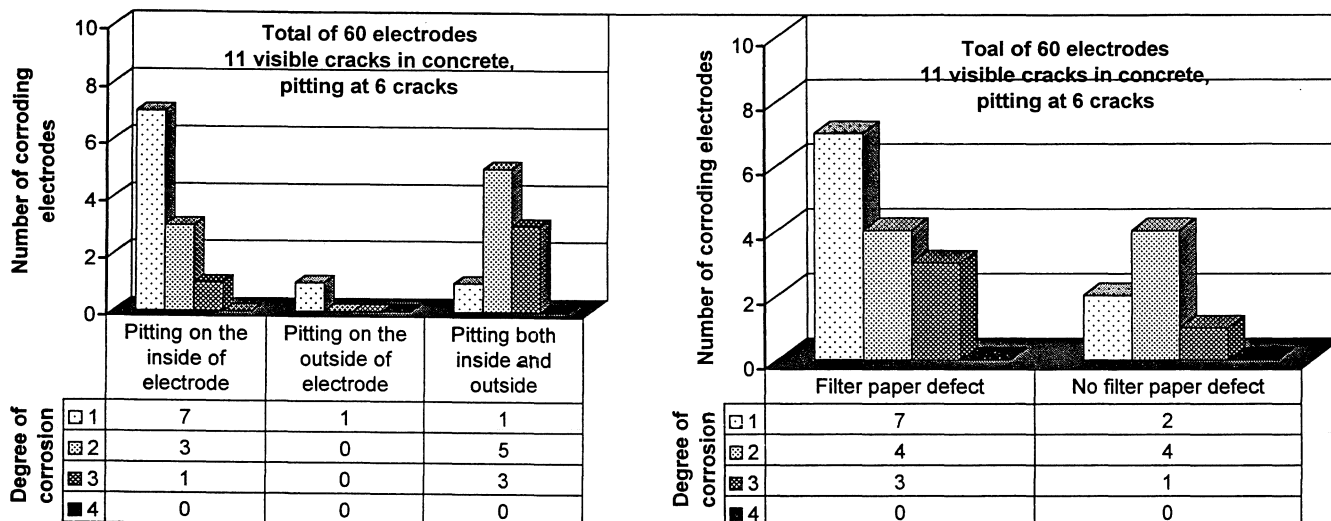


Figure 8. Evaluation of the location of corrosion pits in concrete w/c 0.4 exposed for 2 years in the submerged zone at the Träslövsläge Marine Field Station.

## 6. DISCUSSION

### 6.1 The effect of exposure regime

An evaluation of the effect of the exposure regime is presented in Figure 9. Concrete w/c 0.40 with plain sulfate resisting portland cement, sulfate resisting portland cement and 5 % silica fume, or slag cement were exposed to all exposure regimes. Figure 9 shows the percentage of electrodes corroding with pitting on the inside of electrodes, on the outside of electrodes, or with pitting on both the inside and the outside of electrodes.

As indicated in Figure 9, the corrosion activity was generally found to be very low in concrete exposed submerged in the laboratory at +5 °C or at room temperature, as compared to concrete exposed in all other exposure regimes. The results from wetting and drying in the laboratory at room temperature seems to be more representative for the field performance as compared to concrete exposed submerged in the laboratory at +5 °C or at room temperature.

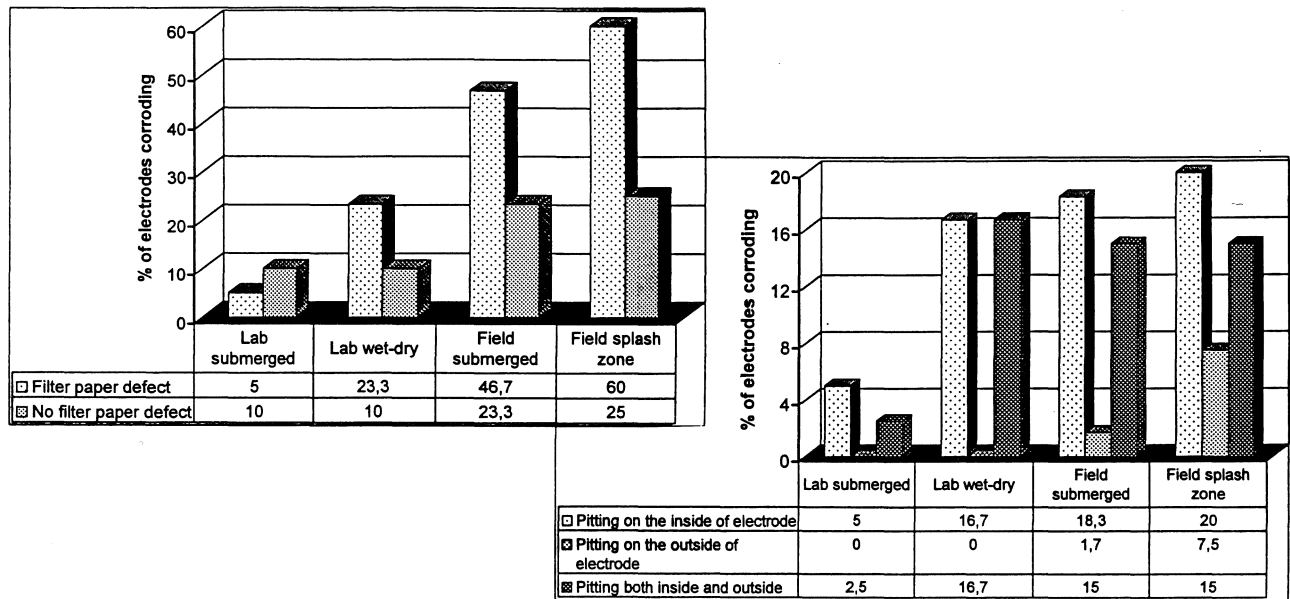


Figure 9. The effect of exposure regime on the corrosion activity for all concrete with w/c 0.40.

## 6.2 the effect of artificial filter paper defects and compaction voids or cracks

The incorporation of artificial filter paper defects at the steel – concrete interface had a strong negative effect on the resistance to corrosion. except for electrodes in concrete exposed submerged in the laboratory, as shown in Figure 9.

34 of a total of 210 examined electrodes in all concrete exposed exhibited evidence on visible compaction voids or cracks at the steel surface. 16 electrodes or approximately 50 % of the electrodes with visible compaction voids or cracks at the steel surface also experienced pitting corrosion. However, only approximately 25 % of the electrodes with visible compaction voids or cracks at the steel surface corroded in concrete exposed submerged in the laboratory.

The effect of microstructural defects in the concrete seems to be far more important in concrete exposed to moisture- and temperature variations, as compared to concrete submerged at a constant temperature in the laboratory. The visible compaction voids or cracks and the artificially produced filter paper defects at the steel surface had relatively little effect on the resistance to corrosion initiation in concrete submerged at a constant temperature in the laboratory. These findings support the idea that it is not the defects, but the effects of the defects on the moisture variations at the depth of the reinforcement, and the temperature variations, which control the chloride threshold. The positive effect of introducing silica fume seems to be related to the improvement of the homogeneity and the reduced permeability of the cover, which in turn reduces the moisture variations at the depth of the reinforcement. This effect can of course also be achieved by increasing the cover thickness or by lowering the w/c ratio.

### 6.3 The effect of bending of steel

In all exposure tests, corrosion was initiated in the deformed parts at the inside of the U-bend steel electrodes in approximately 70 % of the corroding electrodes. The bending of hot rolled black steel is likely to cause cracking of the scale and roughening of the steel surface in the deformed zone, and especially so in the more narrow inside of the U-bend steel electrodes.

### 6.4 The effect of cement type and exposure temperature

The use of slag cement had a strong negative effect on the resistance to pitting corrosion, except for slag cement concrete exposed submerged in the laboratory at + 5 °C, as compared to the use of SRPC with 0 or 5 % silica fume in the binder. The net effect considering all exposure regimes is illustrated in Figure 10. However, it should be noted that the slag cement concrete also exhibited more visible cracks or voids at the steel – concrete interface, as illustrated in Figure 11. The results nevertheless indicate that slag is more sensitive to the formation of cracks, and that the effect of cracks on the resistance to pitting corrosion is more negative for slag cement as compared to SRPC with 0 or 5 % silica fume in the binder.

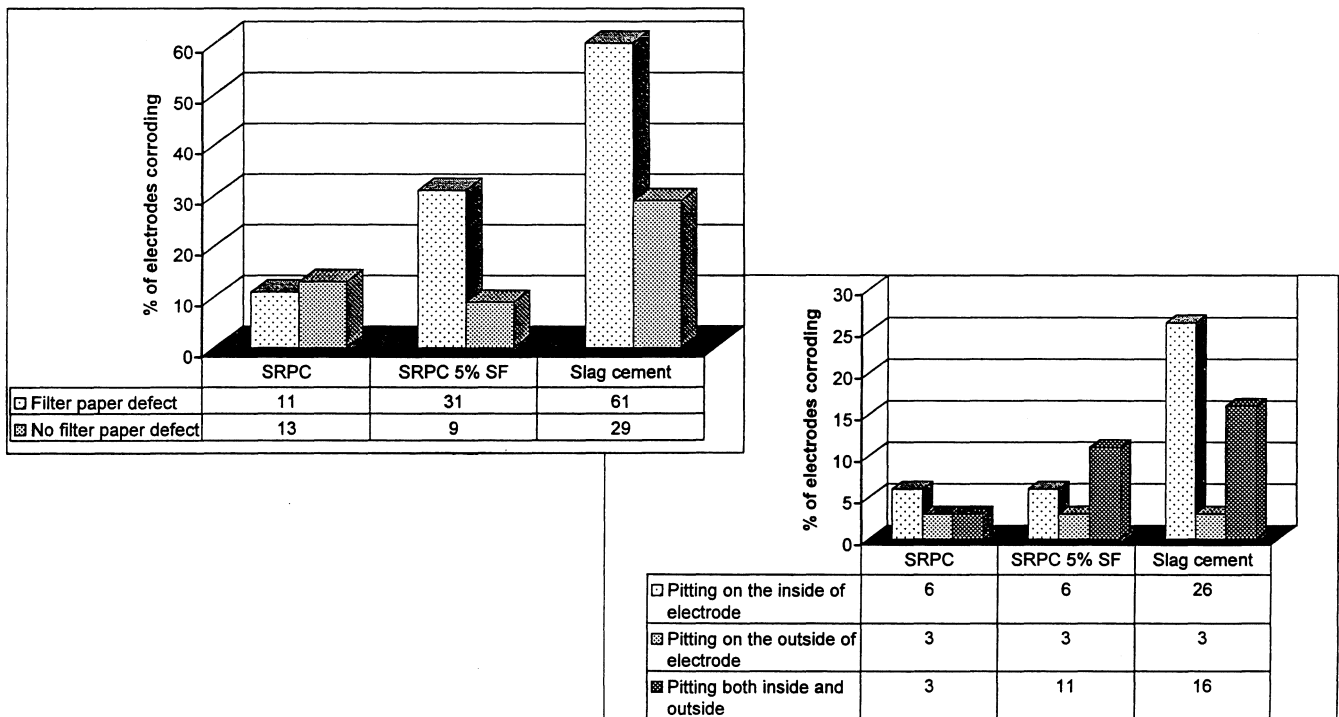


Figure 10. The effect of binder composition on the resistance to pitting corrosion

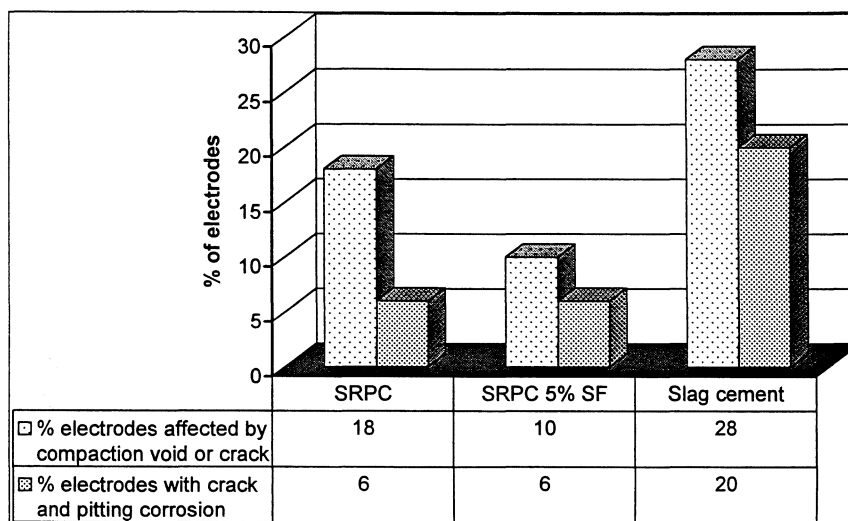


Figure 11. The effect of binder composition and compaction voids or cracks at the steel – concrete interface on the resistance to pitting corrosion

## References

1. Sandberg, P. "Factors affecting the chloride threshold levels for uncracked reinforced concrete exposed in a marine environment – Part I: Field exposure tests of reinforced concrete". To be published in *Adv. Cem Bas Mat.*
2. Sandberg, P. "Factors affecting the chloride threshold levels for uncracked reinforced concrete exposed in a marine environment – Part II: Laboratory- and field exposure of corrosion cells". To be published in *Adv. Cem Bas Mat.*
3. Glass, G.K.; Buenfeld, N.R. "Chloride threshold levels for corrosion induced deterioration of steel in concrete". In *Chloride Penetration into Concrete*; Nilsson, L-O; Ollivier J.P., Eds.; RILEM Publications, France, 1997, pp 429-440.
4. Yonezawa, T.; Ashworth, V.; Procter, R. P. M. "Pore solution composition and chloride effects on the corrosion of steel in concrete". *Corrosion Engineering* 1988, 44, No. 7, 489-499.
5. Page, C. L.; Treadaway, K. W. J. "Aspects of the electrochemistry of steel in concrete". *Nature* 1982, 297, 109-115.

6. Mammoliti, L. T.; Brown, L. C.; Hansson, C. M.; Hope, B. B. "The influence of surface finish of reinforcing steel and pH of the test solution on the chloride threshold concentration for corrosion initiation in synthetic pore solutions". *Cem. & Concrete Res.* 1996, 26, No. 4, 545-550.
7. Pettersson, K. "Service Life of Concrete Structures - In saline environment". CBI Report 3:96. Swedish Cement and Concrete Research Institute, Stockholm 1996.
8. Sandberg, P. "Critical evaluation of factors affecting chloride initiated reinforcement corrosion in concrete". Report TVBM-3068, Lund Institute of Technology, Building Materials, 1995.
9. Tuutti, K. "Chloride induced corrosion in marine concrete structures". In *Durability of Concrete in Saline Environment*; Sandberg, P., Ed.; Cementa and Aalborg Portland, Uppsala, Sweden, 1996, pp 81-93.
10. Tuutti, K. "Corrosion of steel in concrete". CBI Fo 4:1982. Swedish Cement and Concrete Research Institute, Stockholm 1982.
11. Arup, H.; Sørensen, H. E. "A proposed technique for determining chloride thresholds". In *Chloride Penetration into Concrete*; Nilsson, L-O; Ollivier J.P., Eds.; RILEM Publications, France, 1997, pp 460-469.
12. ACI Committee 309. "Guide for consolidation of concrete". ACI 309R-87. In *ACI Manual of Concrete Practice*; Detroit, Mich. 1990.
13. NT BUILD 443. In *Concrete, hardened: Accelerated chloride penetration, part 6.4.4 Profile grinding*.
14. Tang, L.; Sandberg, P. "Chloride penetration into concrete exposed under different conditions" In *Durability of Building Materials and Components 7, II*; Sjöström, C., Ed.; E & FN Spon, London, 1996; pp 453-461.

# APPENDIX A

*Calculated chloride thresholds presented as total chloride content by weight of binder*





**Table A1.** Chloride thresholds expressed as % total Cl by weight of binder, measured in concrete/mortar corrosion cells exposed submerged in a 16 % NaCl solution in the laboratory.

				Steel potentials (mV rel MnO <sub>2</sub> )									
Cell Label	Mix No.	Defects	Exp. temp. °C	free pot.	-450 mV	-350 mV	-250 mV	-200 mV	-150 mV	-100 mV	-50 mV	0 mV	+50 mV
A-PC0.50	1	no	+ 20	1.2 2.1	>3.0 >3.0	>3.0 >3.0	>3.0 >3.0	2.5 3.0	2.0 1.7	2.3 1.7	1.8 1.2	1.6 1.9	1.5 1.8
				Steel potentials (mV rel MnO <sub>2</sub> )									
Cell Label	Mix No.	Defects	Exp. temp. °C	free potential		-450 mV	-350 mV			-100 mV	+50 mV		
B-PC0.41	2	no	+ 20	2.2	1.9	>3.0 >3.0	>3.3	>3.3		>3.0 >3.0	1.7 >3.0		
B-PC0.41	2	yes	+ 20	0.5	>3.3	>3.0 >3.0	>3.3	>3.3		>3.0 >3.0	1.9 >3.0		
C-PC0.41	2	no	+ 5	>2.0	>2.0	>2.0 >2.0	>2.0	>2.0	>2.0		1.8 >2.0	>2.0 >2.0	
C-PC0.41	2	yes	+ 5	>2.0	>2.0	>2.0 >2.0	>2.0	>2.0	>2.0		>2.0 >2.0	>2.0 >2.0	
D-SF0.42	3	no	+ 5	>1.2	>1.2	>1.2 >1.2	>1.2	>1.2	>1.2		>1.2 >1.2	>1.2 >1.2	
D-SF0.42	3	yes	+ 5	>1.2	>1.2	>1.2 >1.2	>1.2	>1.2	>1.2		>1.2 >1.2	>1.2 >1.2	
E-SL0.40	4	no	+ 5	>1.0	>1.0	>1.0 >1.0	>1.0	>1.0	>1.0		>1.0 >1.0	>1.0 >1.0	
E-SL0.40	4	yes	+ 5	>1.0	>1.0	>1.0 >1.0	>1.0	>1.0	>1.0		>1.0 >1.0	>1.0 >1.0	
F-mortPC	5	no	+ 5	>1.7 >1.5 >1.3 >1.1	>0.9 >0.7 >0.5	N.A N.A N.A	-	>1.7 >1.5 >1.3 >1.1	>0.9 >0.7 >0.5	N.A N.A N.A	-	-	

**Table A2.** Chloride thresholds expressed as % total Cl by weight of binder, measured in concrete corrosion cells exposed to cycles of 2 hours wetting and 22 or 166 hours drying in a 16 % NaCl solution in the laboratory at room temperature.

		Steel potentials (mV rel MnO <sub>2</sub> )											
		12 hrs wetting - 6½ days drying					12 hrs wetting - 12 hrs drying						
		Free potential				-350 mV		Free potential				-350 mV	
Cell Label	Mix No.	Filter paper defects				Filter paper defects		Filter paper defects				Filter paper defects	
		Yes	No	Yes	No	Yes	No	Yes	No	Yes	No		
<b>K-PC0.41</b>	<b>2</b>	>0.6	>0.6	>0.6	>0.6	-	-	0.4	>0.6	>0.6	>0.6	-	>0.6
		>0.6	>0.6	>0.6	>0.6			>0.6	>0.6	>0.6			
		>0.6		>0.6				>0.6		>0.6			
<b>L-SF0.42</b>	<b>3</b>	>0.6	>0.6	>0.6	>0.6	-	-	0.5	>0.7	>0.7	>0.7	-	>0.7
		>0.6	>0.6	>0.6	>0.6			>0.7	>0.7	>0.7			
		>0.6		>0.6				>0.7		>0.7			
<b>M-SL0.40</b>	<b>4</b>	nil	nil	nil	nil	-	-	nil	nil	nil	>0.8	-	>0.8
		nil	>1.0	nil	>1.0			nil	>0.8	nil			
		nil		nil				nil		nil			

">" indicates that no corrosion was seen within the test period. The figure indicates the total chloride content at the depth of the steel electrode.

"nil" indicates that corrosion was initiated within a week after the start of chloride exposure.

**Table A3.** Chloride thresholds expressed as % total Cl by weight of binder, measured in concrete corrosion cells exposed at the Träslövsläge Marine Field Station.

		Steel potentials (mV rel MnO <sub>2</sub> )											
		Submerged						Splash zone					
		Free potential				-350 mV		Free potential				-350 mV	
Cell Label	Mix No.	Filter paper defects				Filter paper defects		Filter paper defects				Filter paper defects	
		Yes	No	Yes	No	Yes	No	Yes	No	Yes	No		
O-subPC0.41	2	0.7	>2.2	>2.2	>2.2	>2.2	>2.2	-	-	-	-	-	-
		1.6	>2.2	>2.2	>2.2	>2.2	>2.2	-	-	-	-	-	-
		>2.2	>2.2	>2.2	>2.2	>2.2	>2.2	-	-	-	-	-	-
		>2.2	>2.2	>2.2	>2.2	>2.2	>2.2	-	-	-	-	-	-
P-splaPC0.41	2	-	-	-	-	-	-	0.7	1.1	0.6	1.0	>1.8	>1.8
		-	-	-	-	-	-	1.0	0.8	1.1	1.3	>1.8	>1.8
		-	-	-	-	-	-	0.5	0.6	1.3	0.8	-	-
		-	-	-	-	-	-	1.1	0.9	1.1	1.2	-	-
R-subSF0.42	3	0.3	>1.9	>1.9	0.8	1.4	>1.9	-	-	-	-	-	-
		0.8	1.0	>1.9	>1.9	1.2	>1.9	-	-	-	-	-	-
		0.7	0.9	1.3	1.0	-	-	-	-	-	-	-	-
		>1.9	1.3	>1.9	>1.9	-	-	-	-	-	-	-	-
S-splaSF0.42	3	-	-	-	-	-	-	>0.9	>0.9	>0.9	>0.9	>0.9	>0.9
		-	-	-	-	-	-	0.9	>0.9	>0.9	>0.9	>0.9	>0.9
		-	-	-	-	-	-	0.7	>0.9	>0.9	>0.9	>0.9	>0.9
		-	-	-	-	-	-	>0.9	>0.9	>0.9	>0.9	>0.9	>0.9
T-subSL0.40	4	0.2	>0.7	>0.7	>0.7	0.2	>0.7	-	-	-	-	-	-
		0.3	0.5	>0.7	>0.7	0.6	>0.7	-	-	-	-	-	-
		>0.7	>0.7	0.4	>0.7	-	-	-	-	-	-	-	-
		0.3	>0.7	0.6	>0.7	-	-	-	-	-	-	-	-
U-splaSL0.40	4	-	-	-	-	-	-	0.1	0.2	0.2	0.4	0.5	>0.6
		-	-	-	-	-	-	0.3	>0.6	0.3	>0.6	0.5	>0.6
		-	-	-	-	-	-	0.3	0.5	0.5	>0.6	-	-
		-	-	-	-	-	-	0.4	0.5	0.5	>0.6	-	-

">" indicates that no corrosion was seen within the test period. The figure indicates the total chloride content at the depth of the steel electrode.

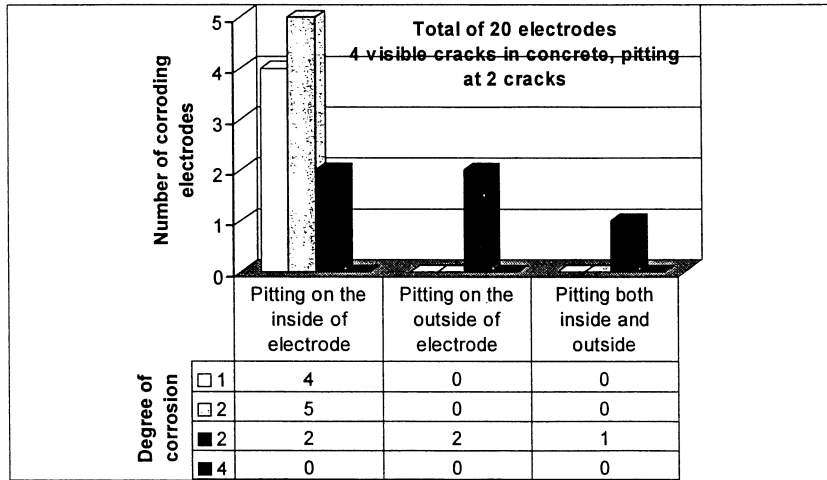


# APPENDIX B

*Compilation of results on the effects of defects at the steel-concrete interface, the exposure regime, and the cement type, on the chloride threshold*

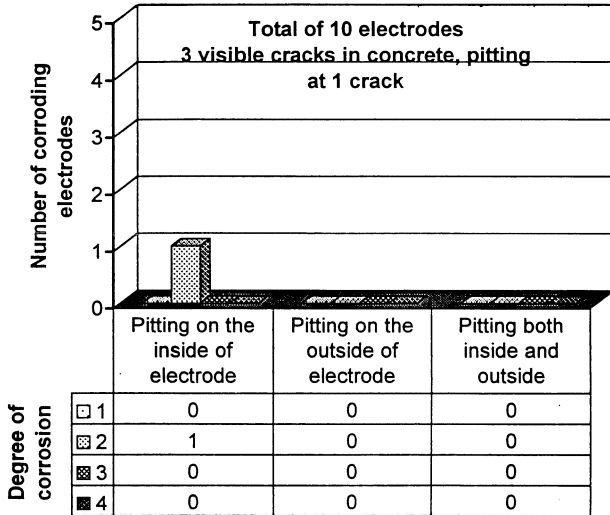


Lab SRPC 0.50 submerged

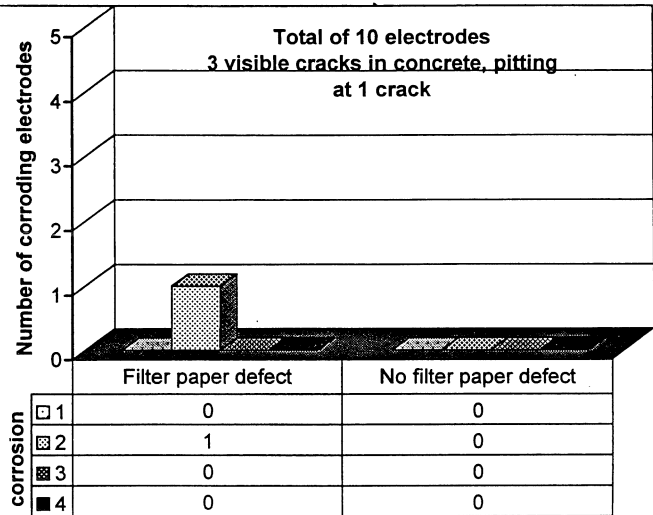




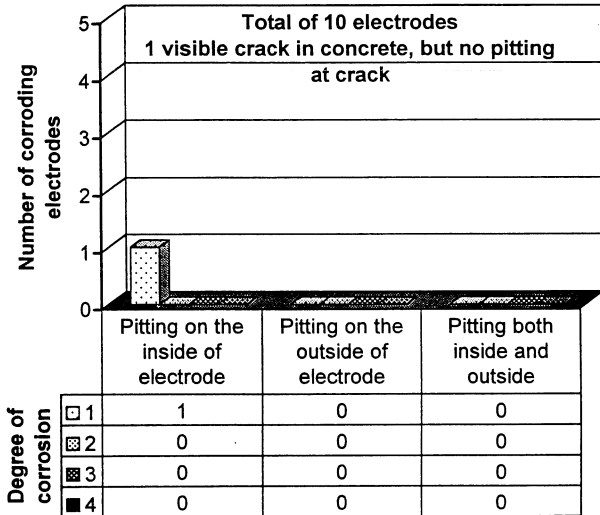
Lab SRPC wet-dry



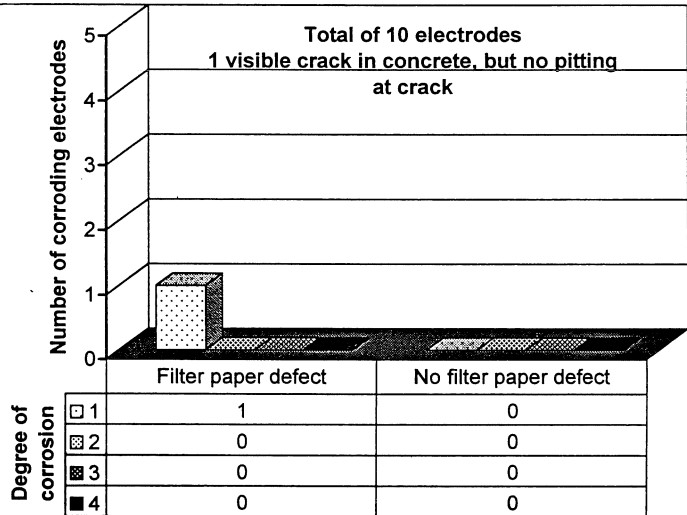
Lab SRPC wet-dry



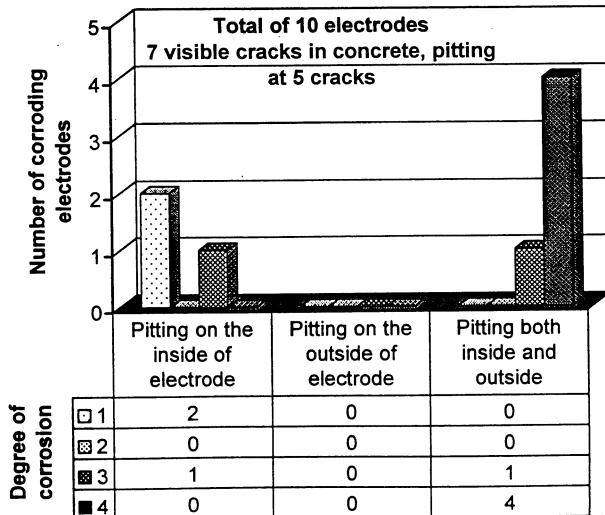
Lab SRPC 5%SF wet-dry



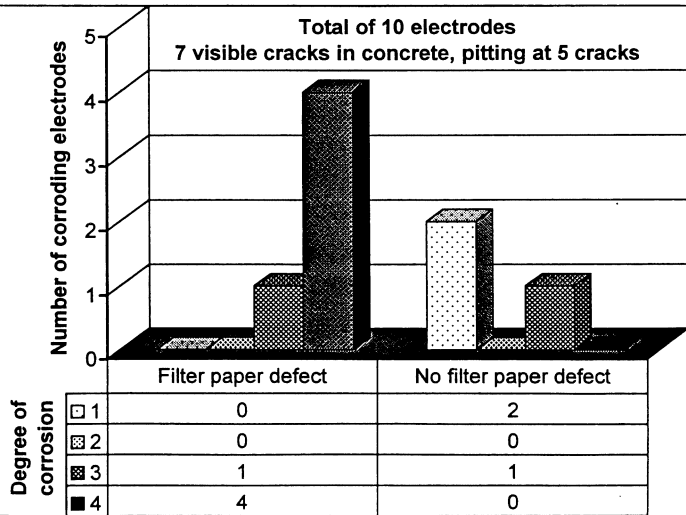
Lab SRPC 5% SF wet-dry



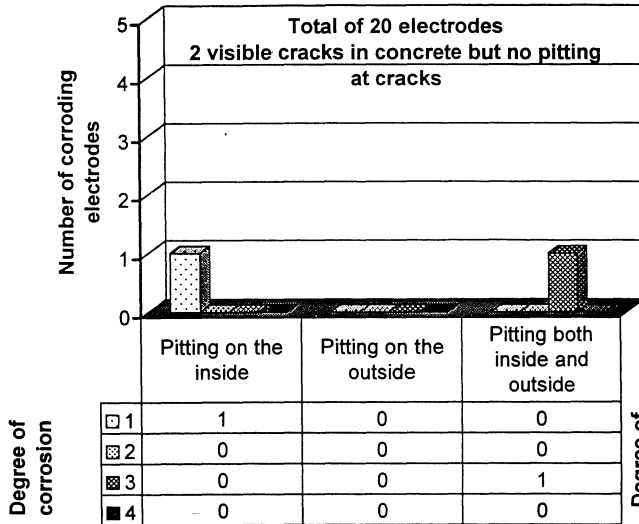
Lab slagcem wet-dry



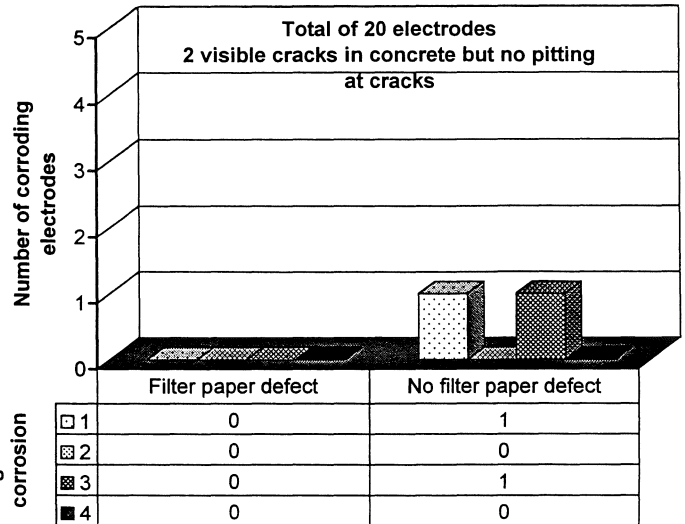
Lab slagcem wet-dry



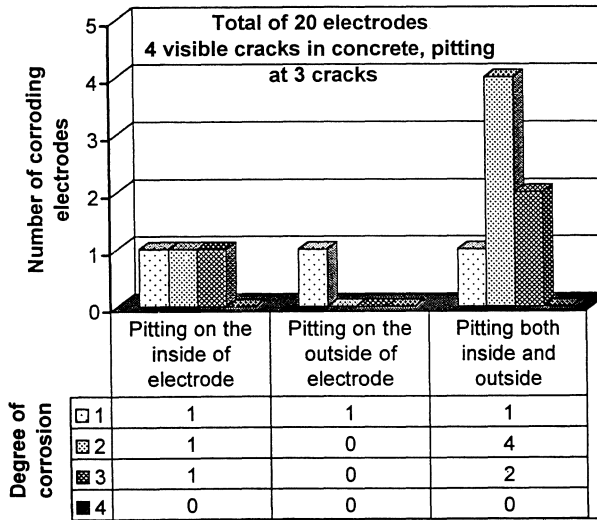
Träslövläge SRPC submerged



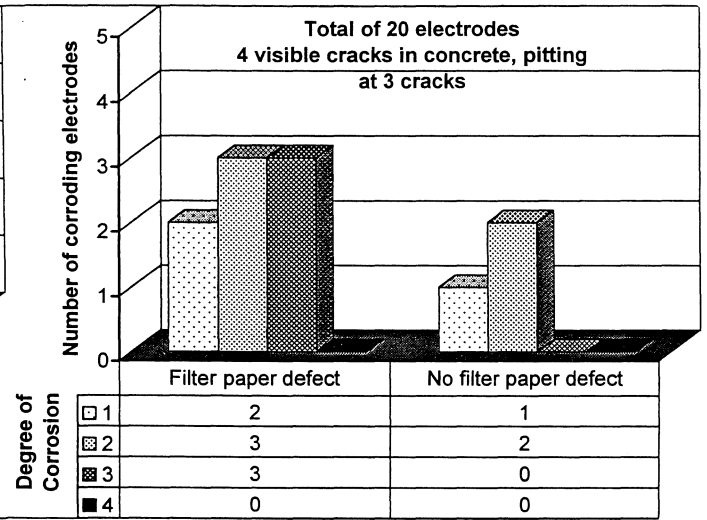
Träslövläge SRPC submerged



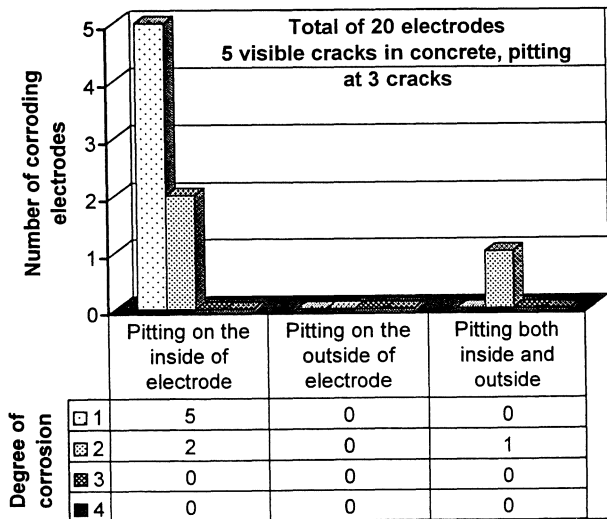
Träslövläge SRPC 5% SF submerged



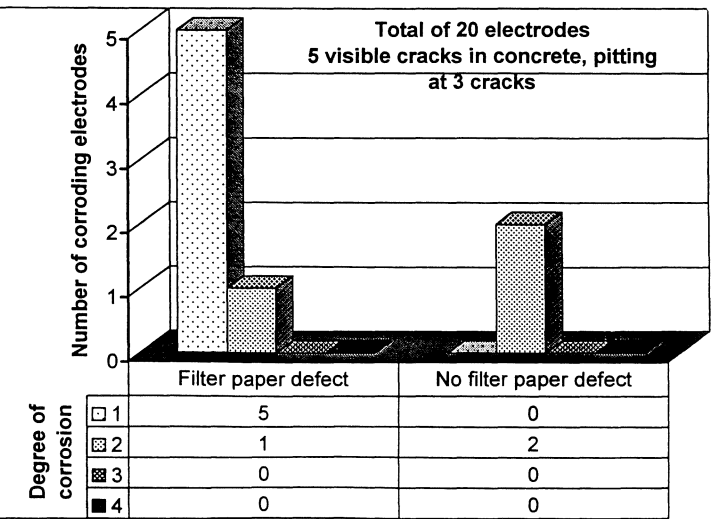
Träslövläge SRPC 5% SF submerged



Träslövläge slag submerged



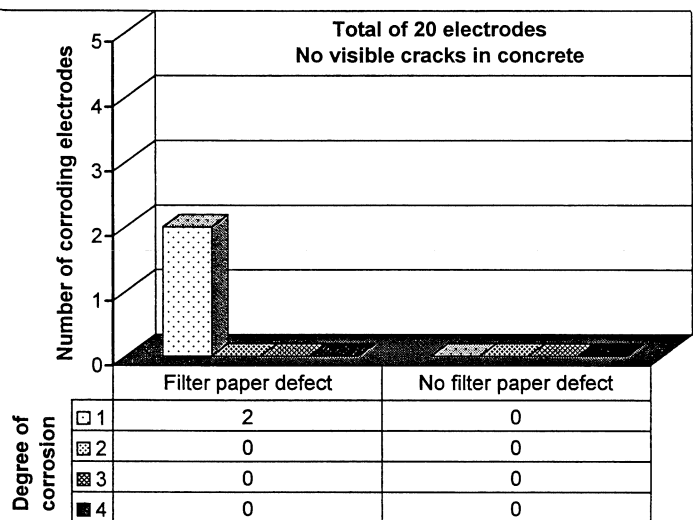
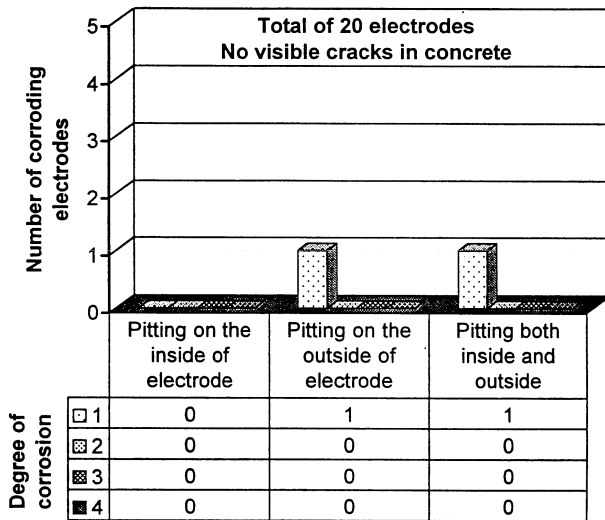
Träslövläge slag submerged



The concrete corrosion cell "Träslövsläge SRPC splash zone – P-spla PC0.41" (marked L 596-19) was lost into the sea in the winter of 1996-97.

Träslövsläge SRPC 5%SF splash zone

Träslövsläge SRPC 5% SF splash



Träslövsläge slag splash zone

Träslövsläge slag splash zone

